ISSN 1061-3862, International Journal of Self-Propagating High-Temperature Synthesis, 2021, Vol. 30, No. 2, pp. 100–105. © Allerton Press, Inc., 2021.

Thin $Zn_{1-x}Mn_xO$ Films (x = 1–4 at %) by Chemical Bath Deposition: Influence of Dopant Concentration

G. R. Patil[a], M. B. Shelar[b, *], N. J. Kambale[a], L. D. Kadam[a], V. S. Raut[a], and B. N. Pawar[c]

[a] *Department of Physics, Dr. Patangrao Kadam Mahavidyalaya, Ramanandnagar, Sangli (affiliated to Shivaji University), Maharashtra, India*

[b] *Thin Film Materials Laboratory, Department of Physics, D.Y. Patil College of Engineering and Technology, Kolhapur (affiliated to Shivaji University), Maharashtra, India*

[c] *Department of Physics, Bharati Vidyapeeth Deemed University, Yashwantrao Mohite College, Pune, Maharashtra, India*

**e-mail: maheshshelar29@gmail.com*

Received January 10, 2021; revised February 27, 2021; accepted March 3, 2021

Abstract—Thin films of $Zn_{1-x}Mn_xO$ (x = 1–4 at %) were applied onto a glass substrate by low-cost chemical bath deposition (CBD). The films were characterized by XRD, UV–VIS absorption spectra, SEM, and vibrating sample magnetometry—with special emphasis on the influence of dopant concentration x. Structural and optical properties of deposited films imply that the Mn^{2+} ions substituted Zn^{2+} ions without changing the wurtzite structure of ZnO. No impurity phases were detected in XRD patterns. The band gap in ZnO was found to increase with increasing x. Magnetic measurements showed that Mn-doped ZnO samples exhibited ferromagnetic behavior at room temperature, which tentatively was associated with the replacement of Zn^{2+} ions by Mn^{2+} ions in the ZnO lattice.

Keywords: thin Mn-doped ZnO films, chemical bath deposition (CBD), optical properties, ferromagnetism

DOI: 10.3103/S1061386221020096

1. INTRODUCTION

Over the past two decades, diluted magnetic semiconductor materials have attracted much attention as an excellent media in which both the charge (electron and holes) and spin related phenomena take place in a one and the same substance, which is an important property for spintronic devices [1]. Due to a large exciton binding energy of ZnO, some zinc ions can be replaced by magnetic ions capable of ferromagnetic coupling [2]. Among other transition metals, ZnO doping with Mn seems most encouraging because Mn has a highest possible magnetic moment [3], and the first half of the *d*-band is fully occupied, thus promoting the formation of a stable fully polarized state. In addition, Mn is isomorphic to Zn and exhibits variable oxidation state and acceptor properties in a ZnO matrix since the ionic radius of Zn^{2+} (0.74 Å) is smaller than that of Mn^{2+} (0.80 Å) and larger than that of Mn^{3+} (0.66 Å).

There are continuing efforts to elucidate the origin of the observed ferromagnetism in Mn-doped ZnO [4] and the Mn^{2+}-induced room-temperature ferromagnetism and spin-glass behavior in hydrothermally grown Mn-doped ZnO nanorods [5] where the ferromagnetic ordering got stabilized upon an increase in hole concentration. Wojnarowicz et al. [6] studied the structural and magnetic properties of Co–Mn co-doped ZnO nanoparticles obtained by microwave solvothermal synthesis. Yan et al. [7] described Mn-doped ZnO nanorod arrays prepared by CVD method with ferromagnetic ordering above room temperature. Droubay et al. [8] synthesized Mn-doped ZnO epitaxial thin films at different temperatures and achieved room temperature ferromagnetism in the samples synthesized at 950°C. Sample preparation and annealing effects on the ferromagnetism in Mn-doped ZnO can be found in [9].

To date, bulk samples and thin films of Mn-doped ZnO have been prepared by different methods such as sol–gel [10], radiofrequency magnetron sputtering [11], pulsed laser deposition [12], and spray pyrolysis [13]. Ferromagnetism in different $(ZnO)_{1-x}(MnO_2)_x$ systems still remains controversial and the magnetic properties of oxide films were found highly sensitive to preparation method [14, 15].

In this communication, we report on the preparation of thin $Zn_{1-x}Mn_xO$ films (x = 1–4 at %) by low-cost chemical bath deposition (CDD) method and their characterization, with special emphasis on the influence of dopant concentration x.

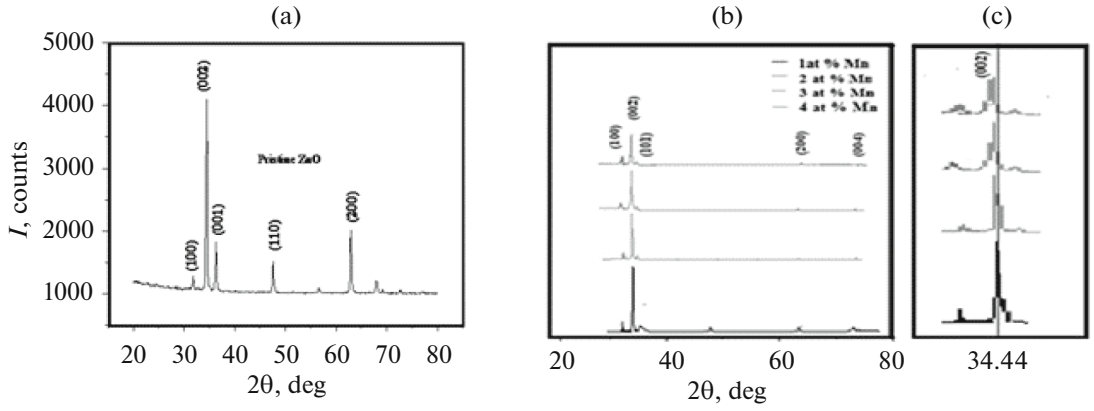

Fig. 1. XRD patterns of undoped (a) and Mn-doped $Zn_{1-x}Mn_xO$ films with different x (indicated), and (c) resolved (002) peak revealing its shift; film thickness 100–150 nm, annealing at 65–85°C for 2 h.

2. EXPERIMENTAL

CBD method is based on heating the alkaline (pH 10.3) bath of zinc salt. Zinc nitrate $Zn(NO_3)_2 \cdot 2H_2O$ and manganese nitrate $Mn(NO_3)_2 \cdot 2H_2O$ were used as a source of Zn and Mn, respectively. Each formula unit contained one Mn^{2+} cation and two NO^{3-} anions. Starting solution was prepared by dissolution of 0.08 M zinc nitrate in deionized water. To this solution, varied amounts of manganese nitrate were added and pH was adjusted to 10.3 with aqueous solution of ammonia. Dopant concentration was varied between 1.0 and 4.0 at %. Prior to deposition, glass substrates were cleaned with acetone, isopropyl alcohol, and triply distilled water successively for 15 min each in an ultrasonic sonicator and finally dried with a flux of high-pressure dioxygen. Cleaned glass substrates were immersed in the above alkaline bath heated to 80°C. Heterogeneous reaction on the substrate surface resulted in deposition of Mn-doped ZnO on the substrate surface. The deposition process lasted for 2 h. Deposited films (100–150 nm thick) were annealed in air at 65–85°C for 2 h.

Deposited films were characterized by XRD (Rigaku diffractometer, Cu $K\alpha$ radiation), SEM (JEOL JSM-7001 microscope), absorption spectra (Shimadzu-1800 spectrophotometer), and vibrating sample magnetometry (SQUID magnetometer).

3. RESULTS AND DISCUSSION

3.1. XRD Spectra

The diffraction patterns of undoped and Mn-doped ZnO films are presented in Figs. 1a and 1b. The spectra confirm the crystalline nature of the films: identified (100), (002), (101), (110), (200), and (004) reflections belong to hexagonal ZnO (JCPDS card no. 89-1397).

No other crystalline by-products such as manganese and its oxides were found within the XRD detection limit, thus indicating that the as-prepared thin films have a purely wurtzite structure. This implies that Mn^{2+} ions substituted for Zn^{2+} of the ZnO host without changing the wurtzite structure. The intensity of the (002) plane in pure ZnO film is much stronger than that of Mn-doped ZnO films. With increasing x, the intensity of ZnO (002) peaks is getting weaker, which indicates that the film crystallinity is deteriorated. We also observed a slight shift in position of the (002) peak (Fig. 1c). The weaker intensity and slight shift of the (002) peak may imply that Mn^{2+} incorporates into the ZnO lattice and substitutes the Zn^{2+} site. Similar behavior was also reported by other researchers [16].

Mean crystallite size D was calculated using the Scherrer formula

$$D = k\lambda/\beta\cos\theta, \quad (1)$$

where D is the crystallite size, $k = 0.89$ is a coefficient, β is the full width at half-maximum (FWHM) of diffraction peak, and λ is the wavelength of X-rays. The D values derived from (002) peak widths were estimated as 35.4, 34.1, 32.4, 30.5, and 29.6 nm, respectively. Our XRD results show that Mn doping does not change the wurtzite structure of ZnO for all x. Small (002) peak broadening indicates a decrease in crystal quality in terms preferred grain growth with an increase in Mn content [17].

Figure 2 shows the SEM images of $Zn_{1-x}Mn_xO$ films deposited onto a Si (100) substrate. Instead of transparent oxide glass, silicon was used to achieve better durability of thin film in photovoltaic measurements. In all cases, deposited films have grown in the form of nanorods along the [002] direction. The SEM micrographs also reveal that Mn-doping of ZnO reduces the average crystallite size, which agrees with the XRD results. An increase in x is seen to decrease

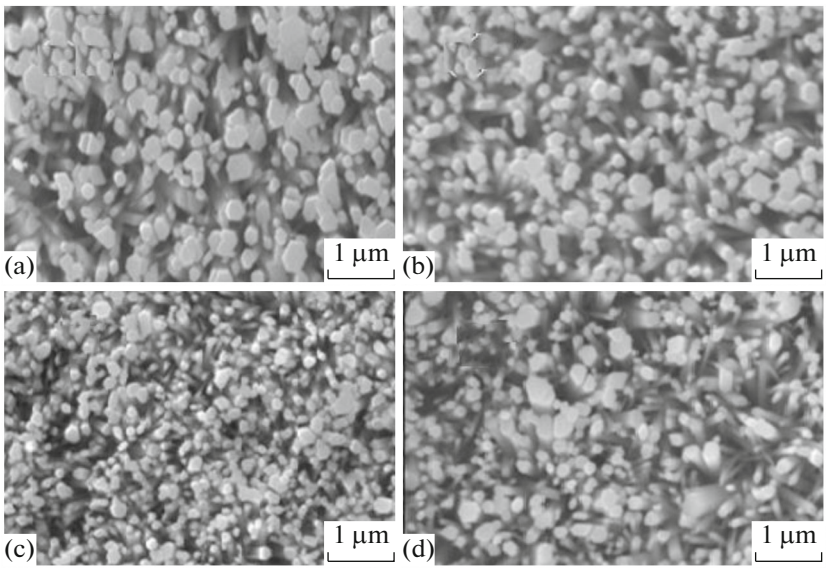

Fig. 2. SEM images of $Zn_{1-x}Mn_xO$ nanorods deposited onto a Si (100) substrate with x = 1.0 (a), 2.0 (b) 3.0 (c), and 4.0 at % Mn (d). Film thickness 100–150 nm, annealing at 65–85°C for 2 h.

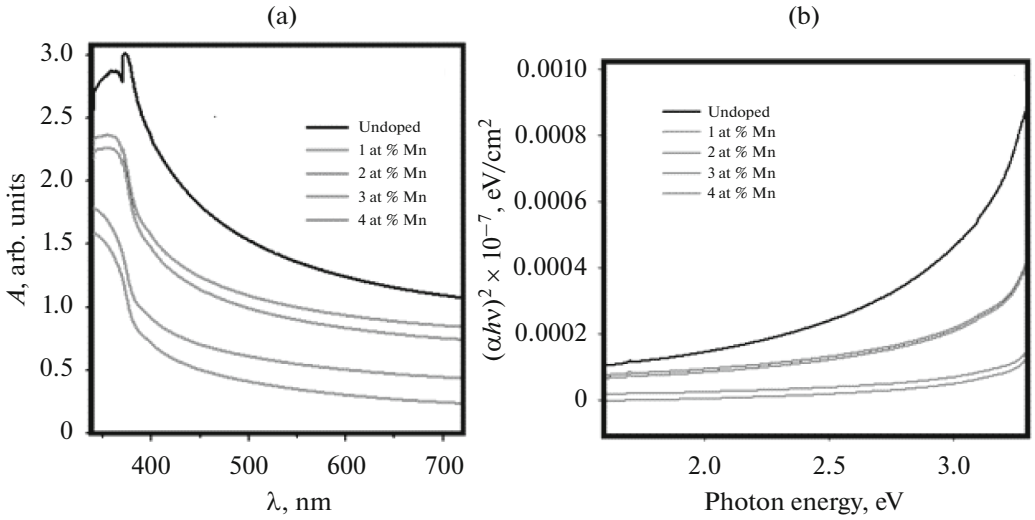

Fig. 3. (a) Absorption spectra and (b) band gap E_g as a function of $h\nu$ for undoped and Mn-doped ZnO films with different x; film thickness 100–150 nm, annealing at.

the diameter of nanorods and increase film randomness.

3.2 Absorption Spectra

Figure 3 presents the absorption spectra and band gaps for undoped and Mn-doped ZnO films with different x. Zinc oxide is a direct band gap material and the energy gap (E_g) can thus be estimated by assuming direct transition between the conduction and valence bands. Theory gives the following relationship between absorption coefficients α and photon energy $h\nu$:

$$\alpha h\nu = A\left(h\nu - E_g\right)^{1/2}. \quad (2)$$

As is seen in Fig. 3a, the absorption edges of $Zn_{1-x}Mn_xO$ films (x = 0–4 at %) are at 450, 430, 410, 3185 and 375 nm, respectively. With increasing x, the absorption edge is seen to shift toward lower wavelengths. Figure 3b shows that band gap E_g grows from 2.8 to 3.2 eV with increasing concentration of Mn^{2+} dopant [18–20]. The blue shift of E_g can be explained in terms of the Burstein–Moss effect [21].This is the phenomenon of which the Fermi level merges into the conduction band upon an increase in carrier concentration, so that the low-energy transitions are blocked.

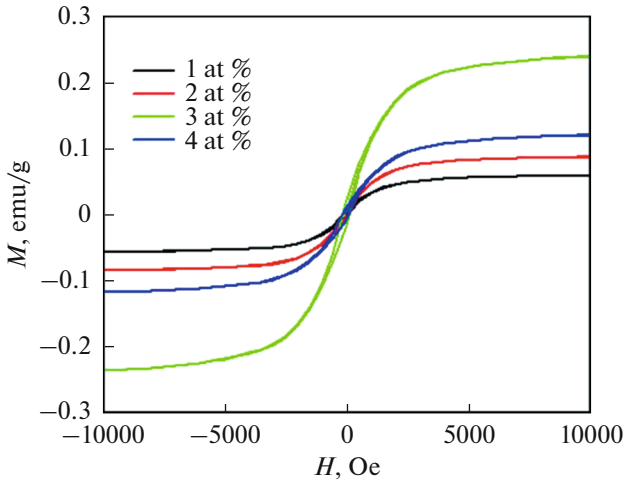

Fig. 4. Hysteresis loops (M–H curves) for $Zn_{1-x}Mn_xO$ films with different x (indicated). Film thickness 100–150 nm, annealing at 65–85°C for 2 h.

Our results are in good agreement with those reported by Sakai and Rekha [22, 23].

3.3. Magnetic Behavior

The room-temperature M–H curves for Mn-doped ZnO thin films under study (Fig. 4) clearly indicate the occurrence of ferromagnetic ordering [24]. Remanent magnetization M_r of $Zn_{1-x}Mn_xO$ films is seen to grow with increasing x. Saturation magnetization M_s attains a value of 0.062, 0.086, 0.24 and 0.238 for x = 1.0, 2.0, 3.0 and 4.0 at %, respectively. These values well agree with the reported ones [25–27].

We have also found that saturation magnetization M_s initially increases up to x = 3.0 and then decreases upon further increase in x, reaching it maximum at x = 3.0. Sharma et al. [27] observed a maximum ferromagnetic moment at x = 2.2 at % in their Mn-doped samples and found that the ferromagnetic ordering decreases with increasing Mn concentration. In our case, we also observed a maximum of M_s at x = 4.0.

Since we did not notice the presence of Mn-related phases in our XRD patterns, it can be concluded that the room-temperature ferromagnetism in our samples is not due to presence of manganese oxides or clusters [28].

Therefore, we consider that the observed room-temperature ferromagnetism most likely is due to the substitution of Mn ions (Mn^{2+}) for Zn ions in the ZnO lattice, which is evidenced by XRD results. According to Ruderman–Kittel–Kasuya–Yosida theory [29, 30], the magnetism originates from the exchange interaction between local spin-polarized electrons (such as the electrons of Mn^{2+}ions) and conduction electrons. This interaction leads to the spin polarization of conductive electrons and subsequently, the spin-polarized conductive electrons undergo exchange interaction with local spin-polarized electrons of other Mn^{2+} ions. Because of the long-range exchange interaction, almost all Mn^{2+} ions exhibit the same spin direction. The conduction electrons are regarded as a medium to "connect" all Mn^{2+} ions. As a result, the material exhibits ferromagnetic behavior [31].

CONCLUSIONS

Thin films of $Zn_{1-x}Mn_xO$ (x = 1–4 at %) were applied onto a glass substrate by low-cost chemical bath deposition (CBD) and characterized by XRD, UV–VIS absorption spectra, SEM, and vibrating sample magnetometry—with special emphasis on the influence of dopant concentration x. XRD results imply that Mn doping does not change the wurtzite structure of ZnO in all samples. Slight (002) peak broadening with an increase in x indicates a gradual growth in crystallite size. Mn doping affects the absorption spectra and optical band gap. For deposited films, saturation magnetization M_s, remanent magnetization M_r, and coercive field H_c (Oe) attain a value of 0.345 emu/g, 0.152 A/m, and 170 kA/m, respectively. Mn doping produces marked influence on the structural, optical, and magnetic properties of ZnO films.

REFERENCES

1. Kazakova, O., van der Meulen, M.I., Petkov, N., and Holmes, J.D., Magnetic properties of single crystalline $Ge_{1-x}Mn_x$ nanowires, *IEEE Trans. Magn.*, 2009, vol. 45, no. 10, pp. 4085–4088. https://doi.org/10.1109/TMAG.2009.2023073

2. Nasir, A., Vijaya, A.R., Zahir, A.K., Tarafder, K., Kumar, A., Wadhwa, M.K., Singh, B., and Ghosh, S., Ferromagnetism from non-magnetic ions: Ag-doped ZnO, *Sci. Rep.*, 2019, vol. 9, 20039. https://doi.org/10.1038/s41598-019-56568-8

3. Shatnawi, M., Alsmadi, A.M., Bsoul, I., Salameh, B., Mathai, M., Alnawashi, G., Alzoubi, G.M., Al-Dweri, F., and Bawa'aneh, M.S., Influence of Mn doping on the magnetic and optical properties of ZnO nanocrystalline particles, *Res. Phys.*, 2016, vol. 6, pp. 1064–1071. https://doi.org/10.1016/j.rinp.2016.11.041

4. Yuan, K., Yu, Q.X., Gao, Q.Q., Wang, J., and Zhang, X.T., A threshold of Vo^{+}/Vo^{++} to room temperature ferromagnetism of hydrogenated Mn doped ZnO nanoparticles, *Appl. Surf. Sci.*, 2012, vol. 258, no. 8, pp. 3350–3353. https://doi.org/10.1016/j.apsusc.2011.08.080

5. Vinod, R., Junaid Bushiri, M., Sajan, P., Achary, S.R., and Sanjose, V.M., Mn^{2+}-induced room-temperature ferromagnetism and spin-glass behavior in hydrothermally grown Mn-doped ZnO nanorods, *Phys. Status*

Solidi A, 2014, vol. 211, no. 5, pp. 1155–1161. https://doi.org/10.1002/pssa.201330394

6. Wojnarowicz, J., Omelchenko, M., Szczytko, J., Chudoba, T., Gierlotka, S., Majhofer, A., Twardowski, A., and Lojkowski, W., Structural and magnetic properties of Co–Mn codoped ZnO nanoparticles obtained by microwave solvothermal synthesis, *Crystals*, 2018, vol. 8, no. 11, 410. https://doi.org/10.3390/cryst8110410
7. Yan, H.L., Zhong, X.L., Wang, J.B., Huang, G.J., Ding, S.L., Zhou, G.C., and Zhou, Y.C., Cathodoluminescence and room temperature ferromagnetism of Mn-doped ZnO nanorod arrays grown by chemical vapor deposition, *Appl. Phys. Lett.*, 2007, vol. 90, no. 8, 082503. https://doi.org/10.1063/1.2460297
8. Droubay, T.C., Keavney, D.J., Kaspar, T.C., Heald, S.M., Wang, C.M., Johnson, C.A., Whitaker, M., Gamelin, D.R., and Chambers, S.A., Correlated substitution in paramagnetic Mn^{2+}-doped ZnO epitaxial films, *Phys. Rev. B*, 2009, vol. 79, no. 15, pp.155203–155208. https://doi.org/10.1103/PhysRevB.79.155203
9. Kluth, O., Schope, G., Hupkes, J., Agashe, C., Muller, J., and Rech, B., Modified Thornton model for magnetron sputtered zinc oxide: Film structure and etching behavior, *Thin Solid Films*, 2003, vol. 442, nos. 1–2, pp. 80–85. https://doi.org/10.1016/S0040-6090(03)00949-0
10. Huang M.H., Mao S., Feick H., Yan H., Wu Y., Kind H., Weber E., Russo R., and Yang P., Room-temperature ultraviolet nanowire nanolasers, *Science*, 2001, vol. 292, no. 5523, pp. 1897–1899, https://doi.org/10.1126/science.1060367
11. Maiti, U.N., Ghosh, P.K., Nandy, S., and Chattopadhyay, K.K., Effect of Mn doping on the optical and structural properties of ZnO nano/micro-fibrous thin film synthesized by sol–gel technique, *Physica B: Condens. Matter*, 2007, vol. 387, nos. 1–2, pp. 103–108. https://doi.org/10.1016/j.physb.2006.03.090
12. Lu, J.G., Huang, K., Zhu, J.B., Chen, X.M., Song, X.P., and Sun, Z.Q., Preparation and characterization of Na-doped ZnO thin films by sol–gel method, *Physica B*, 2010, vol. 405, no. 15, pp. 3167–3171. https://doi.org/10.1016/j.physb.2010.04.045
13. Yılmaz, S., McGlynn, E., Bacaksız, E., Ozcan, Ş., Byrne, D., Henry, M.O., and Chellappan, R.K., Effects of Cu diffusion-doping on structural, optical, and magnetic properties of ZnO nanorod arrays grown by vapor phase transport method, *Appl. Phys.*, 2012, vol. 111, no. 1, pp. 013903-013905. https://doi.org/10.1063/1.3673861
14. Yılmaz, S., Bacaksız, E., McGlynn, E., Polat, İ., and Ozcan, Ş., Structural, optical and magnetic properties of $Zn_{1-x}Mn_xO$ micro-rod arrays synthesized by spray pyrolysis method, *Thin Solid Films*, 2012, vol. 520, no. 16, pp. 5172–5178. https://doi.org/10.1016/j.tsf.2012.04.002
15. Yan, X., Ho, D., Li, H., Li, L., Chong, X., and Wang, Y., Nanostructure and optical properties of M doped ZnO (M = Ni, Mn) thin films prepared by sol–gel process, *Physica B: Condens. Matter*, 2011, vol. 406, no. 20, pp. 3956–3962. https://doi.org/10.1016/j.physb.2011.07.037
16. Yang, S. and Zhang, Y., Structural, optical and magnetic properties of Mn-doped ZnO thin films prepared by sol–gel method, *J. Magn. Magn. Mater.*, 2013, vol. 334, pp. 52–58. https://doi.org/10.1016/j.jmmm.2013.01.026
17. Lee, J.H., Ko, K.H., and Park, B.O., Electrical and optical properties of ZnO transparent conducting films by the sol–gel method, *J. Cryst. Growth*, 2003, vol. 247, nos. 1–2, pp. 119–125. https://doi.org/10.1016/S0022-0248(02)01907-3
18. Deka, S. and Joy, P.A., Synthesis and magnetic properties of Mn doped ZnO nanowires, *Solid State Commun.*, 2007, vol. 142, no. 4, pp. 190–194. https://doi.org/10.1016/j.ssc.2007.02.017
19. Hao, Y.M., Lou, S.Y., Zhou, S.M., Yuan, R.J., Zhu, G.Y., and Hao, N.L., Fabrication and characterization of Mn-doped CuO thin films by the SILAR method, *Nanoscale Res. Lett.*, 2012, vol. 7, p. 100. https://doi.org/10.1186/1556-276X-7-100
20. Gulen, Y., Bayansal, F., Sahin, B., Cetinkara, H.A., and Guder, H.S., Fabrication and characterization of Mn-doped CuO thin films by the SILAR method, *Ceram. Int.*, 2013, vol. 39, no. 6, pp. 6475–6480. https://doi.org/10.1016/j.ceramint.2013.01.077
21. Kharroubi, B., Baghdad, R., Abdiche, A., Bousmaha, M., Bousquet, M., Zeinert, A., Marssi, M.E., Zellama, K., and Hamzaoui, S., Mn doping effect on the structural properties of ZnO-nanostructured films deposited by the ultrasonic spray pyrolysis method, *Phys. Scr.*, 2007, vol. 86, no. 1, 015805. https://doi.org/10.1088/0031-8949/86/01/015805
22. Sakai, K., Kakeno, T., Ikari, A., Shirakata, S., Sakemi, T., Awai, K., and Yamamoto, T., Defect centers and optical absorption edge of degenerated semiconductor ZnO thin films grown by a reactive plasma deposition by means of piezoelectric photothermal spectroscopy, *J. Appl. Phys.*, 2006, vol. 99, no. 4, 043508. https://doi.org/10.1063/1.2173040
23. Rekha, K., Nirmala, M., Nair, M., and Anukaliani, A., Structural, optical, photocatalytic and antibacterial activity of zinc oxide and manganese doped zinc oxide nanoparticles, *Physica B*, 2010, vol. 405, no. 15, pp. 3180–3185. https://doi.org/10.1016/j.physb.2010.04.042
24. Arvind, A., Jayara, M.K., Kumar, M., and Chandra, R., Structural, optical and magnetic properties of Mn doped ZnO thin films prepared by pulsed laser deposition, *Mater. Sci. Eng., B*, 2012, vol. 177, no. 13, pp. 1017–1020. https://doi.org/10.1016/j.mseb.2012.05.005
25. Diaconu, M., Schmidt, H., Hochmuth, H., Lorenz, M., Benndorf, G., Lenzer, J., Spemann, D., Setzer, A.,

Nielsen, K.W., Esquinazi, P., and Grundmann, M., UV optical properties of ferromagnetic Mn-doped ZnO thin films grown by PLD, *Thin Solid Films*, 2005, vol. 486, nos. 1–2, pp. 117–121. https://doi.org/10.1016/j.tsf.2004.11.211

26. Theodoropoulou, N., Misra, V., Philip, J., Leclair, P., Berera, G.P., Moodera, J.S., Satpati, B., and Som, T., High-temperature ferromagnetism in $Zn_{1-x}Mn_xO$ semiconductor thin films, *J. Magn. Magn. Mater.*, 2006, vol. 300, no. 2, pp. 407–411. https://doi.org/10.1016/j.jmmm.2005.05.039
27. Sharma, P., Gupta, A., Rao, K.V., Owens, F.J., Sharma, R., Ahuja, R., Guillen, J.M.O., Johansson, B., and Gehring, G.A., Ferromagnetism above room temperature in bulk and transparent thin films of Mn-doped ZnO, *Nat. Mater.*, 2003, vol. 2, pp. 673–677. https://doi.org/10.1038/nmat984
28. Baik, J.M. and Lee, J.L., Fabrication of vertically well-aligned (Zn,Mn)O nanorods with room temperature ferromagnetism, *Adv. Mater.*, 2005, vol. 17, no. 22, pp. 2745–2748. https://doi.org/10.1002/adma.200500776
29. Ruderman, M.A. and Kittel, C., Indirect exchange coupling of nuclear magnetic moments by conduction electrons, *Phys. Rev.*, 1954, vol. 96, pp. 99–102. https://doi.org/10.1103/PhysRev.96.99
30. Lin, Y.B., Xu, J.P., Zou, W.Q., Lu, L.Y., Lu, Z.H., Zhang, F.M., Du, Y.W., Huang, Z.G., and Zheng, J.G., Effects of annealing and hydrogenation on the properties of ZnMnO polycrystalline films synthesized by plasma enhanced chemical vapor deposition, *J. Phys. D: Appl. Phys.*, 2007, vol. 40, no. 12, 3674. https://doi.org/10.1088/0022-3727/40/12/019
31. Theodoropoulou, N., Misra, V., Philip, J., Leclair, P., Berera, G.P., Moodera, J.S., Satpati, B., and Som, T., High-temperature ferromagnetism in $Zn_{1-x}Mn_xO$ semiconductor thin films, *J. Magn. Magn. Mater.*, 2006, vol. 300, no. 2, pp. 407–411. https://doi.org/10.1016/j.jmmm.2005.05.039